

Anisotropic covalent bonds in KNbO₃ observed by resonant x-ray scattering

E. Mamontov, T. Egami, and W. Dmowski

Department of Materials Science and Engineering and Laboratory for Research on the Structure of Matter, University of Pennsylvania, Philadelphia, Pennsylvania 19104-6272

T. Gog and C. Venkataraman

CMC-CAT, Advanced Photon Source, Argonne National Laboratory, Argonne, Illinois 60439

(Received 3 June 2002; published 10 December 2002)

The resonant x-ray scattering technique was applied to study the directional covalent bonds (orbital ordering) in KNbO₃ associated with ferroelectricity by scanning the incident x-ray energy through the *K* edge of niobium. The orbital ordering was determined by measuring the real part of the x-ray anomalous dispersion f' , with the photon polarization parallel and perpendicular to the orbital ordering vector. The orbital characteristics were assessed through the dependence of f' on the momentum transfer, \mathbf{Q} , since the matrix element for the quadrupolar transition into the *d* states is dependent on \mathbf{Q} , while that for the dipolar transition into the *p* state is not.

DOI: 10.1103/PhysRevB.66.224105

PACS number(s): 77.84.Dy, 78.70.Ck, 78.70.Dm, 78.70.En

I. INTRODUCTION

In the last decade major progress in the theory of ferroelectricity has led to a better understanding of electronic polarization in ferroelectrics due to the directional covalency of the metal-oxygen bonds.¹⁻³ While the directional covalent bonds can be observed by x-ray absorption spectroscopy (XANES),⁴ the orbital character of the bond cannot be determined by XANES. On the other hand, resonant x-ray scattering (RXS) has been successfully applied to determine the orbital and charge ordering in complex oxides such as manganites⁵⁻⁸ and V₂O₃.⁹ The purpose of this work is to apply the resonant x-ray scattering to observe orbital ordering associated with the ferroelectric ordering,¹⁰ by using KNbO₃ as a model system. Ideally, more information on the electronic structure can be obtained through the x-ray inelastic scattering (XIS), but the XIS measurement is extremely time consuming, and requires an extensive setup. The RXS measurement may serve as a preliminary step before the XIS measurement and provide useful information.

Potassium niobate, KNbO₃, is ferroelectric, with a Curie temperature of 708 K (Ref. 11) due to a strong directional bonding between niobium and oxygen. At room temperature KNbO₃ has the structure of orthorhombic symmetry. Strong directional Nb-O bonds are formed in the **a-c** plane, whereas the Nb-O bond along the **b** axis remains nonbonding and largely ionic. The Nb-O bonds form zigzag chains, which are more strongly oriented along the **a** axis, even though the ferroelectric polarization is along the **c** axis. Thus in the present experiment we measured the anisotropic polarization-dependent spectra of absorption and scattering with the photon polarization along **a** and **b** axes. The measurements were performed by scanning the incident x-ray energy through the *K* edge of niobium. By rotating the single crystal around the **c** axis we can make the incident x-ray polarization parallel either to the bonding **a** axis or the nonbonding **b** axis.

In the absorption measurements, the real and the imaginary parts of the anomalous dispersion, f' and f'' , were de-

termined by measuring the absorption coefficient and using the Kramers-Krönig analysis.¹² Both f' and f'' exhibited strong polarization-dependent anisotropy due to components of the Nb-O orbital hybridization along the **a** axis and the lack of such components along the **b** axis. We also measured thermal diffuse scattering to determine the momentum-resolved anisotropy of f' , and compared the results to the averaged f' calculated from the XANES data. The momentum-resolved anisotropy was qualitatively similar to that observed in the absorption measurements, but showed a scattering momentum dependence (shift in energy). It is demonstrated that momentum-resolved resonant x-ray scattering measurements can probe the orbital characteristics of the lowest unoccupied states in the conduction band.

II. RESONANT X-RAY SCATTERING

In an elastic scattering experiment, a photon of energy E_p , momentum \mathbf{q}_1 , and polarization $\boldsymbol{\varepsilon}_1$ scatters from the electronic system in an initial state $|i\rangle$ of energy E_i . The scattered photon has an energy E_p , a momentum \mathbf{q}_2 , and a polarization $\boldsymbol{\varepsilon}_2$. The scattering momentum transfer is $\mathbf{Q} = \mathbf{q}_2 - \mathbf{q}_1$, and $|\mathbf{Q}| = 2|\mathbf{q}_1|\sin\Theta = 2|\mathbf{q}_2|\sin\Theta$, where 2Θ is the scattering angle. The electronic system is left in a final state $\langle f|$ with energy E_f . The total x-ray atomic scattering factor

$$f(\mathbf{Q}, E_p) = f_0(\mathbf{Q}) + f'(\mathbf{Q}, E_p) + if''(\mathbf{Q}, E_p) \quad (1)$$

depends on the incident photon energy E_p , and scattering momentum transfer \mathbf{Q} . Its energy-independent part is^{13,14}

$$f_0(\mathbf{Q}) = \left(\frac{e^2}{mc^2} \right) \langle f | \boldsymbol{\varepsilon}_2 \boldsymbol{\varepsilon}_1 \rho_{\mathbf{Q}} | i \rangle \delta(E_i - E_f), \quad (2)$$

where the density operator

$$\rho_{\mathbf{Q}} = \sum_j e^{i\mathbf{Q}\cdot\mathbf{r}_j} \quad (3)$$

The energy-dependent term (anomalous dispersion) becomes important only when the incident photon energy is tuned to the binding energy of a core state near the absorption edge, that is $E_p \sim E_n - E_i$, since^{13,14}

$$f'(E_p) + if''(E_p) = \left(\frac{e^2}{mc^2}\right) \left(\frac{1}{m}\right) \sum_n \frac{\langle f | \mathbf{P}_{\mathbf{q}_2}^+ \boldsymbol{\varepsilon}_2 | n \rangle \langle n | \mathbf{P}_{\mathbf{q}_1} \boldsymbol{\varepsilon}_1 | i \rangle}{E_n - E_i - E_p + i\Gamma} \delta(E_i - E_f). \quad (4)$$

Here $|n\rangle$ is the intermediate excited state, Γ is the inverse of the lifetime of the state, and the momentum operator is given by

$$\mathbf{P}_{\mathbf{q}} = \sum_j \mathbf{p}_j e^{i\mathbf{q}\cdot\mathbf{r}}. \quad (5)$$

If the intermediate states are anisotropic (for example, due to ferroelectric polarization), this should manifest itself in the anisotropy of both real and imaginary parts of anomalous dispersion.¹⁰ Furthermore, this anisotropy may depend on the photon momentum due to selection of the intermediate states. For instance at the K edge the initial and final states are the $1s$ state, and the matrix element in Eq. (4) is, from Eq. (5),

$$\begin{aligned} \langle n | \mathbf{P}_{\mathbf{q}_1} \boldsymbol{\varepsilon}_1 | i \rangle &\sim \sum_j \langle \varphi(\mathbf{r}) | e^{i\mathbf{q}_1 \cdot \mathbf{r}} \boldsymbol{\varepsilon}_1 \mathbf{p}_j | 1s \rangle \\ &\sim \sum_j \langle \varphi(\mathbf{r}) | e^{i\mathbf{q}_1 \cdot \mathbf{r}} \boldsymbol{\varepsilon}_1 \mathbf{r}_j | 1s \rangle, \end{aligned} \quad (6)$$

where $\varphi(\mathbf{r})$ is the intermediate orbital state, such as p_x , p_y , or $d_{x^2-y^2}$. The exponential terms in the matrix elements can be expanded in a power series, $e^{i\mathbf{q}\cdot\mathbf{r}} = 1 - i\mathbf{q}\cdot\mathbf{r} + (1/2!)(i\mathbf{q}\cdot\mathbf{r})^2 + \dots$, so the matrix elements that have to be considered are the dipolar terms, $\langle p_x | \boldsymbol{\varepsilon} \mathbf{r} | 1s \rangle$ and $\langle p_y | \boldsymbol{\varepsilon} \mathbf{r} | 1s \rangle$, and the quadrupolar term, $\langle d_{x^2-y^2} | (\mathbf{q}\mathbf{r})(\boldsymbol{\varepsilon} \mathbf{r}) | 1s \rangle$. While the dipolar terms are independent of \mathbf{q} , the quadrupolar terms do depend on \mathbf{q} . This difference provides us with the ability to determine the orbital character of the intermediate state, as we show below.

III. EXPERIMENT

A polled single crystal of KNbO_3 , approximately $5 \times 5 \times 5 \text{ mm}^3$ in size, was purchased from GB Group Inc. The faces of the crystal were perpendicular to the orthorhombic axes \mathbf{a} , \mathbf{b} , and \mathbf{c} . Preliminary measurements were carried out at beamline X25 at National Synchrotron Light Source of Brookhaven National Laboratory. Principal part of measurements was performed at the Complex Materials Collaborative Access Team (CMC-CAT) beamline 9ID at the Advance Photon Source (APS) at Argonne National Laboratory. The APS undulator beamline 9ID consists of a double-crystal Si (111) monochromator cooled by liquid nitrogen, a focusing mirror, and a flat harmonic rejection mirror. The incident

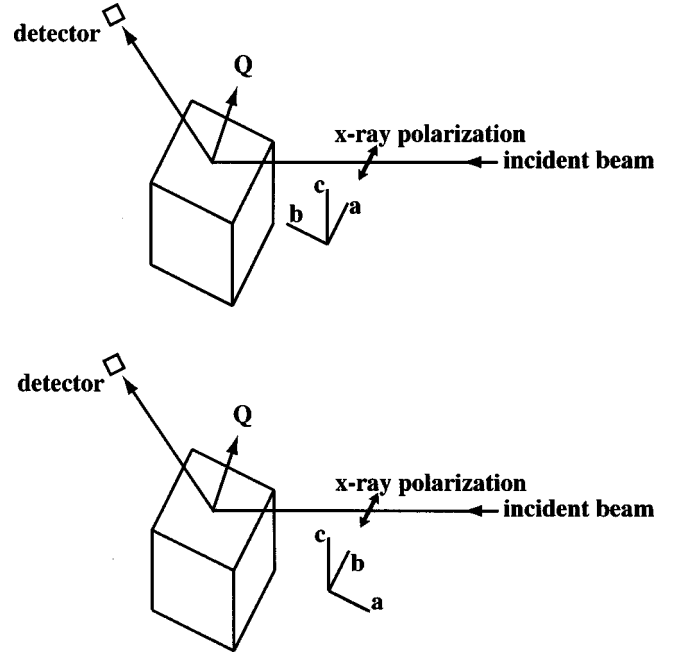


FIG. 1. The setup for the resonant scattering measurements. By rotating the single crystal around the \mathbf{c} axis the same Bragg reflection can be measured with the incident photon polarization parallel either to the bonding \mathbf{a} axis or the nonbonding \mathbf{b} axis.

beam is almost completely linearly polarized. Both the undulator and monochromator were set for the energy near the K edge of Nb (about 18.987 keV). The incident photon energy resolution was about 1.5 eV. For the XANES measurement the single crystal was placed almost perpendicular to the incident beam (the normal to its surface was rotated by 3° away from the beam). The absorption was measured by the fluorescence yield by a detector placed at 3° away from the surface, perpendicular to the incident beam. In this geometry, the change in the penetration depth does not affect the fluorescence yield, thus, self-absorption effects are minimal.^{15,16} We used a Ge solid-state detector with a full width at half maximum resolution of 260 eV at 20 keV, which allowed separating the contribution from Nb K_α fluorescence ($E = 16.568 \text{ keV}$). XANES data were corrected for the detector dead time and normalized to the incident beam intensity measured by the ion chamber.

The setup for the diffraction measurements is shown schematically in Fig. 1. The Bragg reflections along the \mathbf{c} axis, $(0, 0, 8)$, $(0, 0, 10)$, and $(0, 0, 12)$, were measured. By rotating the single-crystal around the \mathbf{c} axis the same Bragg reflection can be measured with the incident photon polarization $\boldsymbol{\varepsilon}$ parallel either to the bonding \mathbf{a} axis or the nonbonding \mathbf{b} axis. In order to determine f' we measured the thermal diffuse scattering (TDS), since the Bragg peaks were highly irregular in shape due to a high Q resolution, which made it difficult to integrate the intensity over the Bragg peaks accurately. For each of the two sample orientations a series of TDS spectra over the same range of \mathbf{Q} were collected at various incident energies near the K edge of Nb. Similar to XANES data, TDS data were corrected for the detector dead time and normalized to the incident beam intensity. The Nb K_β fluores-

cence ($E = 18.791$ keV) could not be resolved directly, so the TDS data were corrected by means of point-to-point subtraction of the Nb K_α fluorescence multiplied by a factor of 0.24 that accounts for the K_α/K_β intensity ratio and the difference in x-ray absorption coefficients for $E(K_\alpha)$ and $E(K_\beta)$.

IV. RESULTS AND DISCUSSION

KNbO_3 has a structure belonging to the perovskite family, and exhibits the same sequence of phase transitions as its isomorphous analog, BaTiO_3 . On cooling from high temperature its cubic symmetry is reduced to tetragonal, orthorhombic, and eventually rhombohedral. Unlike tetragonal BaTiO_3 , KNbO_3 is orthorhombic at room temperature, with the space group $Bmm2$ and the lattice parameters $a = 5.695$ Å, $b = 3.973$ Å, and $c = 5.721$ Å.^{17,18} The **a** and **c** axes are parallel to the pseudocubic (perovskite) face diagonals, and the **b** axis is parallel to the pseudocubic edge. The overall ferroelectric polarization vector is parallel to **c**, the long diagonal of the pseudocubic face, whereas the local Nb-O bonds are in the **a-c** plane and are close to $[101]$ orthorhombic ($[100]$ pseudocubic) direction. The elongation of the **c** axis and the shortening of the **a** axis with respect to the cubic face diagonal result from the displacements of the ferroelectrically active niobium and oxygen ions in the **a-c** plane, as shown in Fig. 2. The niobium-oxygen orbital hybridization in the ferroelectric state is associated with the formation of bonding states in the **a-c** plane. Conversely, the atomic arrangement along the **b** axis (out-of-plane direction in Fig. 2) remains unchanged compared to that in nonferroelectric cubic KNbO_3 , and the Nb-O bond along the **b** axis remains nonbonding (largely ionic).

In order to determine the polarization dependence of the imaginary part of the anomalous dispersion the XANES data obtained with the incident x-ray polarization ϵ , parallel either to the bonding **a** axis or the nonbonding **b** axis, were normalized to the calculated values of f'' (Ref. 19) in KNbO_3 below ($E = 18.950$ keV) and above ($E = 19.050$ keV) the Nb edge. The resulted polarization-dependent f'' exhibits two pronounced anisotropic features as shown in Fig. 3 (bottom). The anisotropy beyond 19.00 keV is due to the atomic structure (crystal field), whereas the difference in the energy range of 18.99–19.00 keV with a peak at 18.995 keV reflects the anisotropic Nb-O bonding. The Nb $1s$ -core electrons can be excited into the antibonding Nb-O states if the incident photon polarization has a component in the **a-c** plane, but not when it is completely parallel to the nonbonding axis **b**. Notably, while the anisotropy of the data beyond $E_p = 19.00$ keV varies with our choice of the high-energy normalization point, that at lower energy is very closely reproducible regardless of the details of the normalization procedure. Expectedly, the polarization-dependent real part of anomalous dispersion obtained by performing the Kramers-Krönig transformation of f'' (Ref. 12) also exhibits anisotropy as shown in the top part of Fig. 3. In particular, there is a crossover between the two spectra at approximately $E_p = 18.995$ keV, where the difference plot changes from negative to positive. Similar to the anisotropy in f'' at $E_p = 18.99$ –19.00 keV, the position of this crossover is inde-

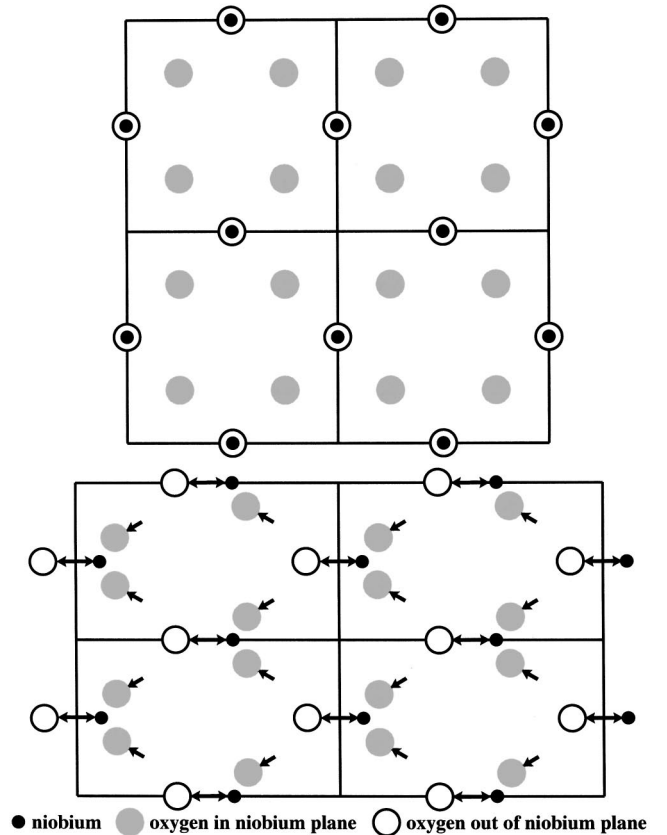


FIG. 2. Niobium-oxygen subsystem in cubic (top) and orthorhombic (bottom) KNbO_3 . The elongation of the **c** axis and the shortening of the **a** axis result from the displacements of the ferroelectrically active niobium and oxygen ions in the **a-c** plane, whereas the atomic arrangement along the out-of-plane **b** axis remains unchanged compared to cubic KNbO_3 .

pendent of the details of the normalization procedure for f'' .

As can be readily seen, the polarization-dependent transition of the Nb $1s$ -core electrons into the anisotropic antibonding Nb-O states manifests itself in both the hump in the $\Delta f''$ plot and the crossover in the $\Delta f'$ plot at the same energy corresponding to the energy of the antibonding states. In the absence of such states (for instance, in cubic KNbO_3 above the Curie temperature) there would be no anisotropy in the anomalous dispersion. In the XANES measurement all transitions of $1s$ -electron into the anti-bonding states of p_x , p_y , and $d_{x^2-y^2}$ symmetries contribute to anisotropy in the f' and f'' . On the other hand, through the resonant x-ray scattering experiment it is possible to vary the relative contribution of the transitions into the states with different orbital characteristics by varying the momentum transfer, and sort them out.

While the determination of f' in the absorption measurements is straightforward, obtaining its values from the resonant x-ray scattering measurements is more difficult. The TDS data processed as described in Sec. III were fitted with a Lorentzian function $y = y_0 + A/[1 + (x - x_0)^2/B^2]$, where parameters x_0 , y_0 , A , and B were allowed to vary. It was necessary to include the background parameter y_0 in order to account for the contribution from fluorescence that varies with the photon energy and was not fully corrected using the

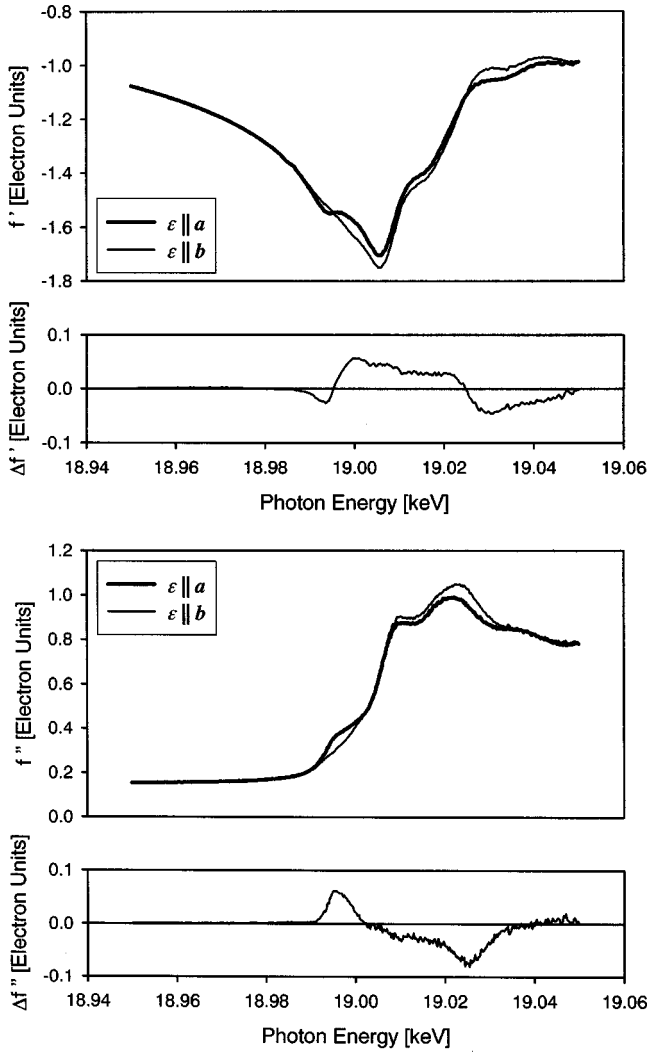


FIG. 3. The real (top) and imaginary (bottom) parts of the x-ray anomalous dispersion near the Nb K edge in KNbO_3 as obtained from XANES (with no momentum resolution). Corresponding difference plots are shown below to emphasize the polarization-dependent anisotropy.

procedure described in Sec. III. Figure 4 presents an example of the fitting the TDS data collected near the $(0, 0, 12)$ Bragg reflection at several photon energies. At particular photon energy, the parameter $A(E_p)$ determined from the fitting is a measure of the scattering intensity expressed in arbitrary units. In order to normalize the data properly, one needs to take into account the energy-dependent absorption, which in a simple symmetrical geometry shown in Fig. 1 reduces the measured scattering intensity by a factor of $0.5/\mu(E_p)$. The absorption coefficient, $\mu(E_p)$, can be obtained merely by normalizing the measured XANES data to the calculated values of $\mu(E_p)$ (Ref. 19) in KNbO_3 below and above the Nb edge. The absorption coefficient determined in such a way is anisotropic following the polarization-dependent anisotropy in XANES data. Then for both polarization directions for each of the three Bragg reflections we performed point-to-point multiplication of $A(E_p)$ by $2\mu(E_p)$ to obtain the scattering intensity $I(E_p)$, which was corrected for absorption,

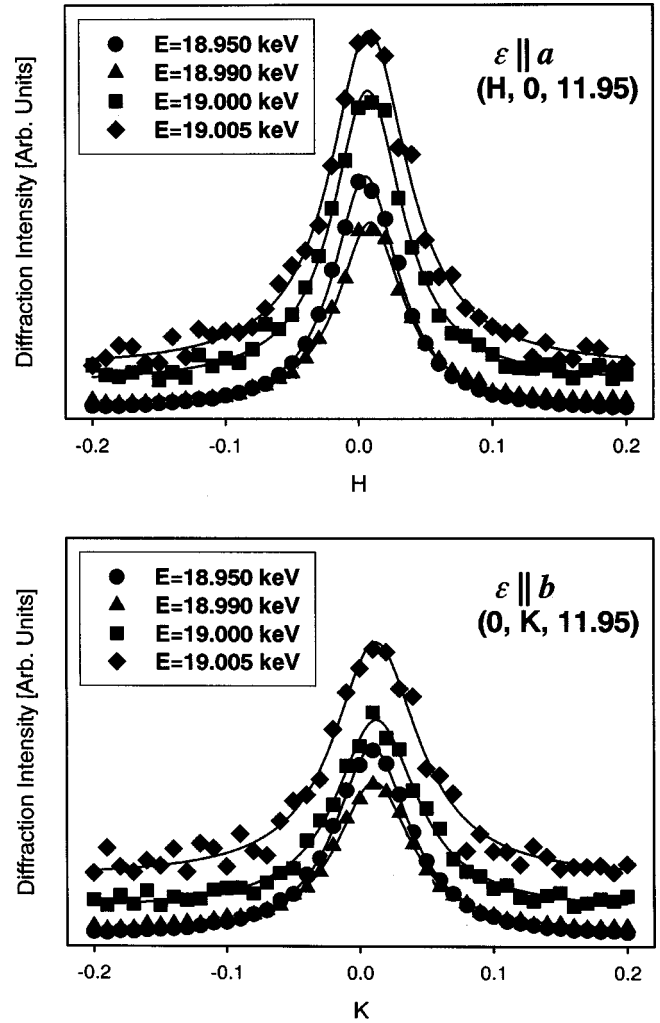


FIG. 4. The thermal diffuse scattering data collected near the $(0, 0, 12)$ Bragg reflection at several photon energies. The lines are fits with four-parameter Lorentzians.

but still expressed in arbitrary units. Finally, in order to express the scattering intensity in the absolute electron units of $(e^2/mc^2)^2$, it is necessarily to normalize the intensity to $|f(\mathbf{Q}, E_p)|^2$ at energies E_1 and E_2 , which are sufficiently away from the edge so that scattering is isotropic. For this purpose, $I(E_p)$ was multiplied by a scaling factor C determined from the equations

$$I(E_1)C = [F_0 + f'(E_1)]^2 + [f''(E_1)]^2, \quad (7)$$

$$I(E_2)C = [F_0 + f'(E_2)]^2 + [f''(E_2)]^2, \quad (8)$$

where F_0 is the energy-independent structure factor of KNbO_3 . We chose $E_1 = 18.950$ keV and $E_2 = 19.050$ keV, for which the calculated¹⁹ values of f' and f'' yield $f'(E_1) = -1.1203$, $f'(E_2) = -0.9925$, $f''(E_1) = 0.1525$, and $f''(E_2) = 0.7828$ for KNbO_3 . Once the measured intensity is expressed in the absolute electron units, the energy dependence of f' could be determined using (1).

The difference plots for f' obtained by subtracting the data collected with $\epsilon \parallel \mathbf{b}$ from those collected with $\epsilon \parallel \mathbf{a}$ are shown in Fig. 5 along with the corresponding anisotropy of

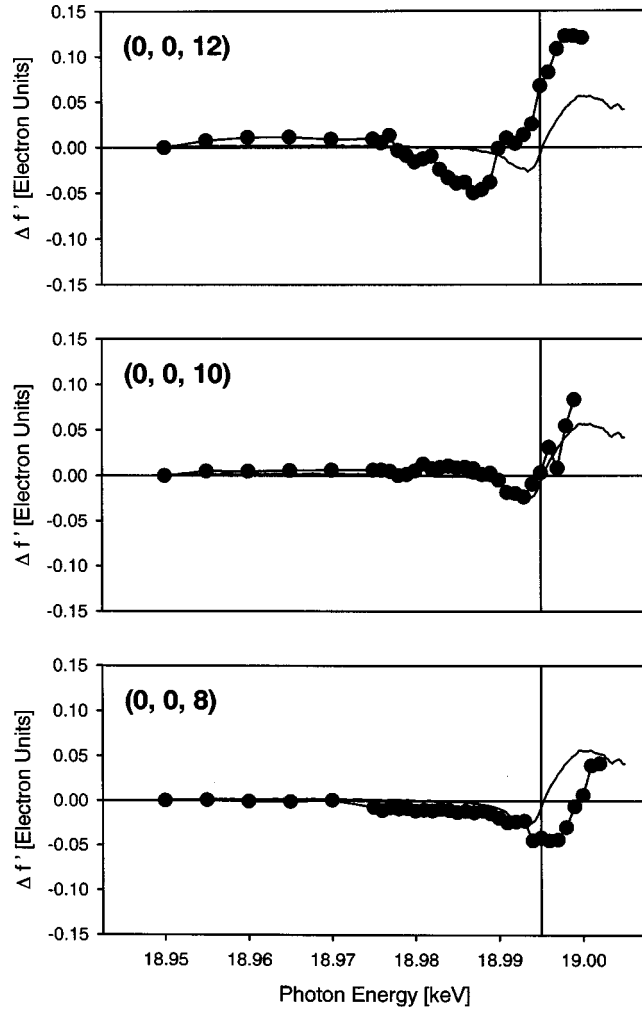


FIG. 5. The difference plots for f' near the Nb K edge in KNbO_3 obtained by subtracting the TDS data collected with $\boldsymbol{\varepsilon} \parallel \mathbf{b}$ from those collected with $\boldsymbol{\varepsilon} \parallel \mathbf{a}$. The corresponding anisotropy of $f'(E_p)$, measured with no momentum resolution by XANES, is shown for comparison as a line with no symbols. The reference line at $E = 18.995$ keV corresponds to the crossover of the $\Delta f'$ obtained by XANES.

$f'(E_p)$ measured with no momentum resolution by XANES. Similarly to the difference plot obtained by XANES, all the diffraction difference plots exhibit a minimum, a crossover, where the difference changes from negative to positive, and a maximum. One can see that the diffraction difference plots exhibit momentum dependence, being shifted downward in energy as Q increases, that is, by increasing Q we access the intermediate states which are lower in energy.

By using expression (6) we can determine the orbital characteristics of the intermediate states through the dependence on Q . The dipolar term for the p orbitals does not depend on the \mathbf{q} , and, therefore, is independent of Q . The relative strength of the quadrupolar transition is parameterized by $qa = q(a_0/Z) = 0.12$, where $q = |\mathbf{q}| = |\mathbf{q}_1| = |\mathbf{q}_2| = 2\pi/\lambda$. Thus only if the intermediate states are predominantly of the d character, the quadrupolar term becomes significant. Considering the orientation of \mathbf{q}_1 , \mathbf{q}_2 , \mathbf{Q} , and $\boldsymbol{\varepsilon}$ with respect to that of the NbO_6 octahedron shown in Fig. 6

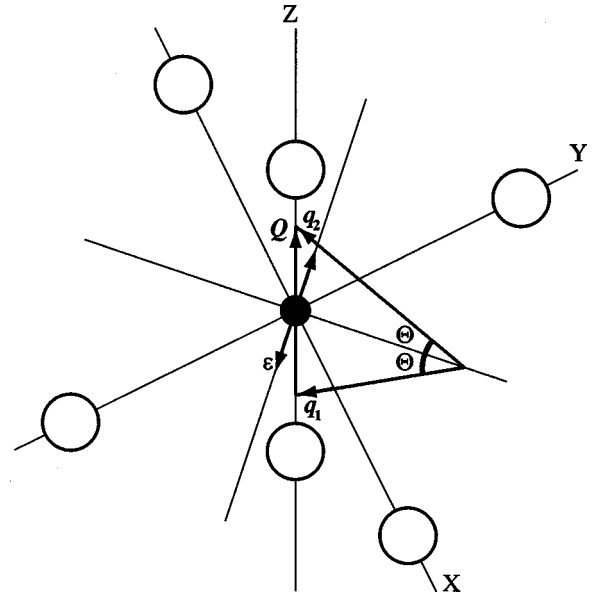


FIG. 6. The orientation of photon polarization and scattering vectors with respect to the NbO_6 octahedron for $\boldsymbol{\varepsilon} \parallel \mathbf{a}$. The angle between \mathbf{q}_1 and \mathbf{q}_2 is denoted 2Θ .

for $\boldsymbol{\varepsilon} \parallel \mathbf{a}$, it is easy to demonstrate that $\langle d_{x^2-y^2} | (\mathbf{q}\mathbf{r}) (\boldsymbol{\varepsilon}\mathbf{r}) | 1s \rangle \sim \sin \Theta$, where 2Θ is the angle between \mathbf{q}_1 and \mathbf{q}_2 defined as $Q = (4\pi/\lambda) \sin \Theta$. Therefore, while anomalous dispersion is usually independent of Q , in the resonant condition when the photon energy E_p corresponds to the energy of the $d_{x^2-y^2}$ orbital hybridized with oxygen p orbitals, it becomes angularly dependent as $[f'(E_p) + if''(E_p)] \sim \sin^2 \Theta$. For Q 's of $(0, 0, 8)$, $(0, 0, 10)$, and $(0, 0, 12)$, corresponding values of Θ are 27° , 35° , and 43° . Thus the contribution of the intermediate d states to resonant scattering increases proportionally to $\sin^2 \Theta$ as 0.21, 0.33, and 0.47, whereas the contribution of the intermediate p states remains unchanged. Consequently the relative contribution of the intermediate states of d character grows with Q . It is known from the local-density approximation calculations of the band structure in KNbO_3 (Ref. 20) that the lowest unoccupied states in the conduction band are of predominantly d character, while those of substantial p character are 3–4 eV above. Therefore, the shift of the characteristic features and the crossover of $\Delta f'(E_p, Q)$ downward in energy with increasing Q must be due to enhancing contribution of the intermediate states of d character. Note that in similar geometry one can expect the shift of $\Delta f'(E_p, Q)$ upward in energy with increasing Q in a compound where the lowest unoccupied states in the conduction band are of p character.

V. CONCLUSION

In this work we used resonant x-ray scattering measurements to study the ferroelectric orbital ordering in a model ferroelectric, KNbO_3 . To probe the hybridized niobium-oxygen states absorption and scattering measurements were performed by scanning the incident x-ray energy through the K edge of niobium. A qualitatively similar polarization-

dependent anisotropy of the real part of the x-ray anomalous dispersion, f' , was observed in both x-ray absorption and resonant scattering measurements. In the latter case, the anisotropy, $\Delta f'(E_p, Q)$, exhibited dependence on the scattering momentum Q , shifting downward in energy as Q increased from $(0, 0, 8)$ to $(0, 0, 10)$ to $(0, 0, 12)$. We concluded that in the geometry we used this shift was due to the increasing relative strength of the quadrupolar transition into the d states that are lower in energy than p states. This measurement demonstrates the possibility of probing the orbital character of the conduction band involved in directional bonds by assessing the scattering momentum dependence of resonant x-ray scattering.

ACKNOWLEDGMENTS

The authors are thankful to H. Krakauer for providing the results of the band structure calculations, and to L. Berman of the X-25 beamline of the National Synchrotron Light Source for most valuable assistance in the measurement. The work at the University of Pennsylvania was supported by the Office of Naval Research through N000-14-01-10860. Use of the Advanced Photon Source was supported by the U.S. Department of Energy, Office of Science, Office of Basic Energy Sciences, under Contract No. W-31-109-ENG-38. The National Synchrotron Light Source is supported by the U.S. Department of Energy Contract No. DE-AC02-98CH10866.

-
- ¹R. E. Cohen, *Nature (London)* **358**, 136 (1992).
²R. D. King-Smith and D. Vanderbilt, *Phys. Rev. B* **47**, 1651 (1993).
³R. Resta, *Rev. Mod. Phys.* **66**, 899 (1994).
⁴For example, B. Ravel, E. A. Stern, R. I. Vedral, and V. Kraizman, *Ferroelectrics* **206–207**, 407 (1998).
⁵Y. Murakami, H. Kawada, H. Kawata, M. Tanaka, T. Arima, Y. Moritomo, and Y. Tokura, *Phys. Rev. Lett.* **80**, 1932 (1998).
⁶Y. Murakami, J. P. Hill, D. Gibbs, M. Blume, I. Koyama, M. Tanaka, H. Kawata, T. Arima, Y. Tokura, K. Hirota, and Y. Endoh, *Phys. Rev. Lett.* **81**, 582 (1998).
⁷K. Nakamura, T. Arima, A. Nakazawa, Y. Wakabayashi, and Y. Murakami, *Phys. Rev. B* **60**, 2425 (1999).
⁸Y. Wakabayashi, Y. Murakami, I. Koyama, T. Kimura, Y. Tokura, Y. Moritomo, K. Hirota, and Y. Endoh, *J. Phys. Soc. Jpn.* **69**, 2731 (2000).
⁹L. Paolasini, C. Vettier, F. de Bergevin, F. Yakhov, D. Mannix, A. Stunault, W. Neubeck, M. Altarelli, M. Fabrizio, P. A. Metcalf, and J. M. Honig, *Phys. Rev. Lett.* **82**, 4719 (1999).
¹⁰T. Egami, in *Fundamental Physics of Ferroelectrics 2000: Aspen Center for Physics Winter Workshop*, AIP Conf. Proc. No. 535, edited by R. E. Cohen (AIP, Melville, NY, 2000), p. 16.
¹¹S. Sawada, S. Nomura, and S. Fujii, *J. Phys. Soc. Jpn.* **13**, 1549 (1958).
¹²For example, D. H. Templeton, in *Handbook on Synchrotron Radiation*, edited by G. S. Brown and D. E. Moncton (Elsevier, Amsterdam, 1991), Vol. 3, p. 205.
¹³M. Blume, *J. Appl. Phys.* **57**, 3615 (1985).
¹⁴P. M. Platzman and E. D. Isaacs, *Phys. Rev. B* **57**, 11 107 (1998).
¹⁵S. Eisebitt, T. Böske, J.-E. Rubensson, and W. Eberhardt, *Phys. Rev. B* **47**, 14 103 (1993).
¹⁶P. Pfalzer, J.-P. Urbach, M. Klemm, S. Horn, M. L. denBoer, A. I. Frenkel, and J. P. Kirkland, *Phys. Rev. B* **60**, 9335 (1999).
¹⁷L. Katz and H. D. Megaw, *Acta Crystallogr.* **22**, 639 (1967).
¹⁸A. W. Hewat, *J. Phys. C* **6**, 2559 (1973).
¹⁹D. T. Cromer, *J. Appl. Crystallogr.* **16**, 437 (1983).
²⁰H. Krakauer (private communication).